Semi-automated segmentation of brain tumor lesions in MR Images.

S. Saraswathy[1], F. Crawford[1], S. J. Nelson[1,2]

[1]Surbeck Laboratory of Advanced Imaging, Department of Radiology, University of California, San Francisco, CA, United States, [2]UCSF/UCB Joint Graduate Group in Bioengineering, University of California, San Francisco, CA, United States

Introduction: Objective, rapid and reproducible methods of measuring tumor volume are of utmost importance to clinicians in assessing the response to treatment and in guiding appropriate therapy for serial studies of brain tumor patients. Assessments of changes in the volume of brain lesions are typically obtained either by visual impression or manually tracing the tumor. Manual segmentation is labor intensive and prone to large variations in intra- and inter-operator performance. While there have been previous reports of automated segmentation, these methods are often computationally intensive and may not be practical for everyday operation. The goal of this study was to implement and validate a relatively simple and rapid method that could be applied to images with different types of contrast and has the potential for not only reducing the variability in measurements, but also the time required to analyze serial changes in lesion volume. Assessment of the "truth" of segmentation is challenging as realistic simulation of MRI data that covers all aspects of clinical data is not yet possible and dissection of actual tissue does not preserve the volume of interest. As the purpose was to replace manual outlining without a measurable effect on the results we performed a validation which determined how accurately manual segmentation agrees with automated results.

Methods: The image to be segmented is first de-noised by filtering it by an anisotropic diffusion filter [1], which preserves edges. This is followed by the calculation of the mean and standard deviation of intensities for all the pixels in a neighborhood around seed points that are selected using an interactive display package developed in our laboratory. This allows definition of a range of intensities around the mean for region growing in terms of the standard deviation σ and two user-input values f_1 and f_2. The pixels around this neighborhood are then checked for inclusion in the region using the following criterion

$$I(x) \in [I_m - f_1\sigma, I_m + f_2\sigma]$$

where $I(x)$ is the intensity value of the pixel at position x. The first iteration is completed after all the valid pixels are included in the region. In the next iteration, mean and standard deviation of the intensity values are recomputed using all the pixels currently included in the region. A new intensity range is calculated from these values and the neighbors of the current region are tested for their inclusion in the region and are added to the region as appropriate. The iterations are continued until no more pixels are added or the maximum number of iterations is reached. The segmentation of hyperintense lesions in FSE-T2 images is known to be a difficult task because the lesions and CSF can have the same intensity values in these images (Fig. 4(a)). We addressed this problem by using the mask obtained by first segmenting CSF from the T1 and then applying it as an exclusion mask.

Results: The algorithm was used to successfully segment hyperintense lesions in FLAIR and T2 images and both hyper-and hypointense lesions separately in T1 contrast enhanced images. Fig 1 shows a 3D view of the segmented lesions on a FSE-T2 image. Fig. 2 shows the volume comparison of the hyperintense lesions on FLAIR images by automated and manual tracing and Fig.3 shows a similar comparison of the results for the contrast enhanced lesion in T1 images for two patients after surgical removal of active tumor. For validating segmentation of FSE images the similarity coefficient [2], which is a measure of overlap between automatically segmented volume and manual segmented data was calculated and was observed to be 81.7 ± 5.88 (n=7). The overlap matrices [2] between the manually and automatically segmented volumes in 30 GlioblastomaMultiformes was found to be 80.09 ± 8.5 for T2 lesions and 74.66 ± 9.31 for contrast enhanced tumors. Time required for the execution of the algorithm was a few seconds per case in a 2.6 GHz Intel Xeon processor.

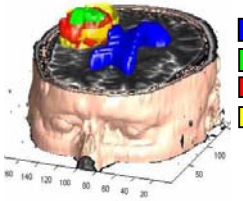

Fig. 1: 3D view of segmented lesions that are thought to correspond to necrosis, edema and tumor

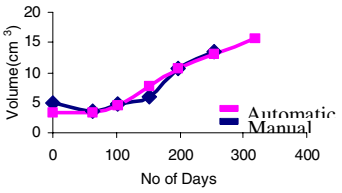

Fig. 2: Volume change of edema in FLAIR image in 6 follow-up studies

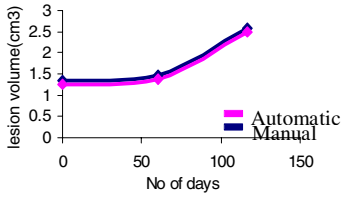

Fig. 3: Volume change of tumor in T1 image in 3 follow-up studies

Discussion: Our findings show that both meningiomas and gliomas can be accurately segmented by means of automated processing, as shown in Fig. 4. Segmentation of lesions with complicated shapes that are difficult to analyze using manual segmentation is possible with this algorithm. In cases where the tumor was very close to the skull or eye region we did a skull stripping prior to running the segmentation which excluded the extraneous objects even before lesion segmentation started. Although we tried refining the segmentation by applying Geodesic level sets [3], the segmentation was not improved considerably. A similar refinement using a fuzzy analysis method [4] was found to increase the computations without considerably improving the segmentation results. For this class of images, we therefore decided to avoid computationally burdensome refinement operations.

Conclusions: The results show that volume measurements obtained using this method are in good agreement with manually segmented data. The implementation of the method is being incorporated as part of the routine evaluation of follow-up data for patients with brain tumors in our institution.

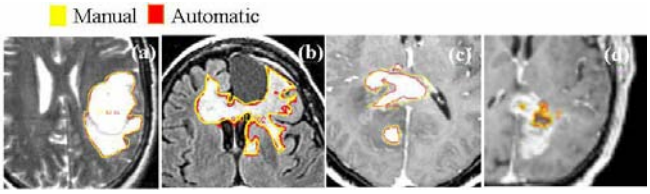

Fig. 4: (a) Segmentation of lesions in FSE T2 image. (b) Segmentation of edema and tumor in FLAIR images. (c) Segmentation of contrast-enhanced lesion in T1 weighted image. (d) Segmentation of the hypointense lesion that is expected to correspond to necrosis in T1 contrast enhanced image

References:

[1] G. Gerig et al., *IEEE trans on Medical Imaging*, 11(2), pp.221-232 (1992).
[2] Zou et al., *Acad Radiol*., 11, pp.178-189 (2004).
[3] V. Caselles et al., *International Journal of Computer Vision*, 22(1), pp.61–79 (1997).
[4] Udupa JK et al., *Graphical Models Image processing*, 58, pp.246-261 (1996).